Annu. Rev. Fluid Mech. 1997. 29:91–122

CONVECTION IN MUSHY LAYERS

M. Grae Worster
Institute of Theoretical Geophysics, Department of Applied Mathematics and Theoretical Physics, University of Cambridge, Silver Street, Cambridge CB3 9EW, United Kingdom

KEY WORDS: solidification, convection, mushy layers, chimneys, stability

ABSTRACT

As a molten alloy or any multi-component liquid is cooled and solidified the growing solid phase usually forms a porous matrix through which the residual liquid can flow. The reactive two-phase medium comprising the solid matrix and residual liquid is called a mushy layer. Buoyancy forces, owing primarily to compositional depletion as one or more of the components of the alloy are extracted to form the solid phase, can drive convection in the layer. In this review, I present an account of various studies of buoyancy-driven convection in mushy layers, paying particular attention to the complex interactions between solidification and flow that lead to novel styles of convective behavior, including focusing of the flow to produce chimneys: narrow, vertical channels devoid of solid. I define an 'ideal' mushy layer and argue that chimneys are an inevitable consequence of convection in ideal mushy layers. The absence of chimneys in certain laboratory experiments is explained in terms of nonideal effects.

1. INTRODUCTION

Solidification is a process that has only recently captured the attention of the fluid-mechanics community. Yet, as illustrated in a review by Huppert (1990), a wide range of fluid-mechanical phenomena can occur as a direct consequence of the solidification of a liquid melt. Additionally, the flow of melt in the vicinity of a growing solid can have profound consequences for the structure and composition of the solidified product (Langlois 1985, Davis 1990, Hurle 1992). Many interesting and important interactions between solidification and fluid flow take place while the solid and liquid are separated by a geometrically simple interface, such as a planar or gently curved interface. Such cases can be described mathematically using the usual equations of fluid flow (the Navier–

0066-4189/97/0115-0091$08.00

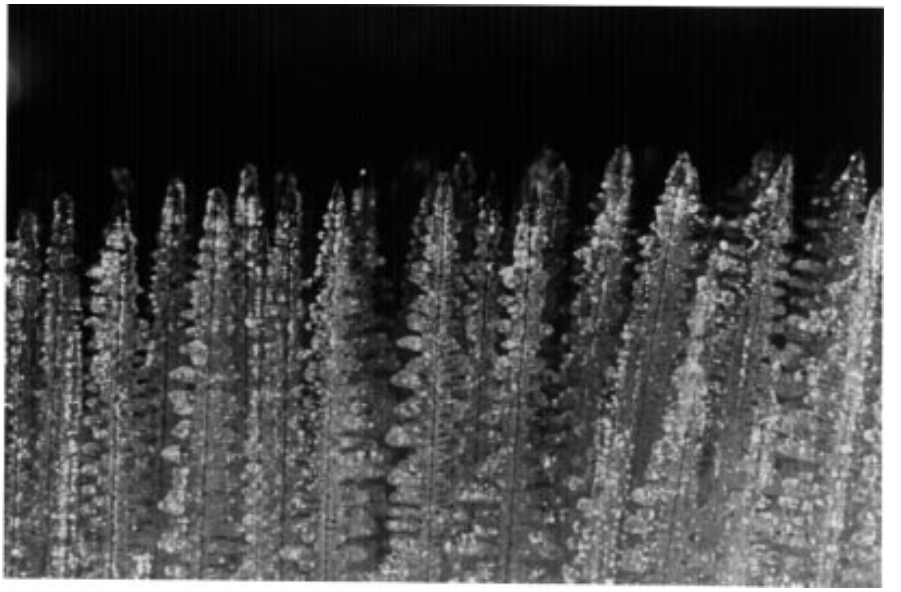

Figure 1 A close-up photograph of a mushy layer grown from an aqueous solution of ammonium chloride showing the individual dendrites that make up the solid matrix. The typical spacing between the dendrites shown is about 0.5 mm, while the depth of the mushy layer is a few centimeters.

Stokes equations) and of heat and mass transfer. The main novelty and interest lie in determining the evolution of the solid–liquid interface, which is a free boundary. For example, in many situations, the interface is found to be morphologically unstable (Mullins & Sekerka 1964) and in practice becomes highly convoluted within a "mushy layer" (Figure 1) in which solid and liquid are intermingled in close proximity. Many fluid-mechanical studies have analyzed the effects of various types of flow of the melt on the criteria for morphological instability (Glicksman et al 1986, Davis 1990). These have been motivated in part by a quest to discover means of suppressing instability and hence of producing single crystals of higher quality for the semiconductor industry.

Rather less attention has been paid to fluid flow within mushy layers. Yet such layers are ubiquitous in systems that solidify in the natural environment and are, therefore, not subject to the careful controls used to produce single crystals industrially. They are also common in large alloy castings, whose structural quality can be severely impaired by the effects of fluid flow within the mushy layer during production.

The fluid mechanics of mushy layers is quite different from that of wholly molten regions. In essence, a mushy layer is a porous medium (Phillips 1991)

through which the interstitial melt can flow. However, the permeability structure of the mushy layer is not known in advance but must be calculated simultaneously with solving the coupled equations of heat, mass, and momentum transport. Fascinating and unsuspected interactions can occur between solidification and flow within mushy layers. These are the subject of this article, in which I describe some of the fluid-mechanical predictions that have been made of the evolution of mushy layers and discuss how these relate to experimental measurements and observations made in a variety of industrial and environmental situations.

Although flow in mushy layers can be driven by a variety of mechanisms, most attention has been paid to natural, buoyancy-driven convection. Natural convection during solidification can be driven by two agents: the melt is inevitably cooled in order for it to solidify, and the consequent temperature gradients give rise to thermal convection; in addition, if the melt is a mixture (alloy) of different components, then compositional convection can be driven by gradients in concentration generated in the melt as one or more of the components are preferentially incorporated into the solid. Even given the very simple geometry of a melt being cooled at an upper or a lower horizontal boundary, six different fluid-mechanical regimes are possible, depending on the different combinations of thermal and compositional buoyancy (Huppert & Worster 1985). Here I focus on the single case of a two-component liquid cooled from below to form a solid leaving a less-dense residual liquid. This seemingly narrow focus nevertheless encompasses many of the fluid-mechanical phenomena peculiar to mushy layers. To fix ideas, we can think of an aqueous salt solution being cooled from below to form a mushy layer comprising a matrix of solid salt crystals bathed in residual solution such as that shown in Figure 1. In this situation, a one-dimensional, vertically stratified state is possible in which the compositional buoyancy is destabilizing and the thermal buoyancy is stabilizing.

This combination of stable thermal buoyancy and unstable compositional buoyancy can lead to convection in the form of double-diffusive fingers in the liquid region (Turner 1979, 1985). However, within the mushy layer the temperature and concentration of the liquid are strongly coupled (as described below) and the buoyancy field is typically dominated by the concentration field, so no double-diffusive effects occur there.

In this review, I define and discuss the behavior of what might be termed an "ideal" mushy layer. The ideal mushy layer has a fluid phase that is isotropic and Boussinesq. The solid in an ideal mushy layer forms a stationary rigid matrix, whose permeability is locally isotropic and a function only of the local void fraction (but see caption of Figure 2). Above all, the solid and liquid phases in an ideal mushy layer are in perfect, local thermodynamic equilibrium. Of course, the ideal mushy layer is a theoretical construct, but there is much experimental

evidence that many real mushy layers conform closely to the predicted behavior of the ideal. There is experimental evidence, too, that some mushy layers behave differently from the ideal. In such cases, the theoretical predictions of the evolution of ideal mushy layers provide a useful basis for comparison by which the physical reasons for the nonconformity can be elucidated.

One of the most striking consequences of natural convection in mushy layers is the formation of "chimneys". These are narrow, essentially vertical vents, devoid of solid, from which emanate plumes of buoyant, salt-depleted solution (Figure 2). Much of this article is focused on the natural convection within mushy layers that is responsible for the formation of chimneys, though other types of convection are described as well.

Chimneys have most commonly been studied in the laboratory by solidifying aqueous solutions of ammonium chloride (see, for example, Copley et al 1970, Chen & Chen 1991, Tait et al 1992). There is also evidence of chimneys in metallic castings (Sarazin & Hellawell 1988), and recent experiments carried out by JS Wettlaufer, HE Huppert, and myself have revealed chimneys forming in mushy layers of ice grown from sea water. In Figure 2, I show additional evidence of chimneys in a mushy layer of ice crystals grown from a mixture of water and isopropanol. However, chimneys have failed to appear in many laboratory experiments using other aqueous salt solutions (Huppert 1990). This is an indication that modifications may be required to the theory of ideal mushy layers if all experimental observations are to be understood.

We begin in Section 2 by defining an ideal mushy layer and describing the equations that govern its evolution. Then, in section 3, the different modes of convection in the liquid and mushy regions that can occur during solidification

Figure 2 (*a*) A shadowgraph image of buoyant plumes emanating from chimneys in a mushy layer. The mushy layer is the black region at the bottom of the photograph and was about 9 cm deep when the photograph was taken. The solid phase of the mushy layer is ice growing from a mixture of water and isopropanol. The residual liquid in the mushy layer is enriched in isopropanol, is therefore less dense than the overlying liquid mixture and escapes through chimneys to form the plumes shown in the photograph. Photographs (*b*) and (*c*) are taken in plan view of the tops of mushy layers, showing chimney vents. The solid phase in (*b*) comprises crystals of ammonium chloride grown from aqueous solution, whereas the solid phase in (*c*) comprises ice crystals grown from a mixture of water and isopropanol. Evidently, chimneys can occur in mushy layers of very different internal morphology. In both cases the diameters of the chimneys are about 2–3 mm, as indicated by the rulers in the photographs. It is noteworthy that the spacing between chimneys in mushy layers of ammonium chloride is comparable to the depth of the layer, whereas the spacing between the chimneys in the mushy layer of ice shown in (*c*) is about one fifth of the depth of the layer. This is likely to be a consequence of the fact that the permeability in the latter case is more strongly orthotropic: the permeability to flow in the vertical direction is larger than the permeability in horizontal directions. This nonideal feature of mushy layers has not yet received much attention.

(a)

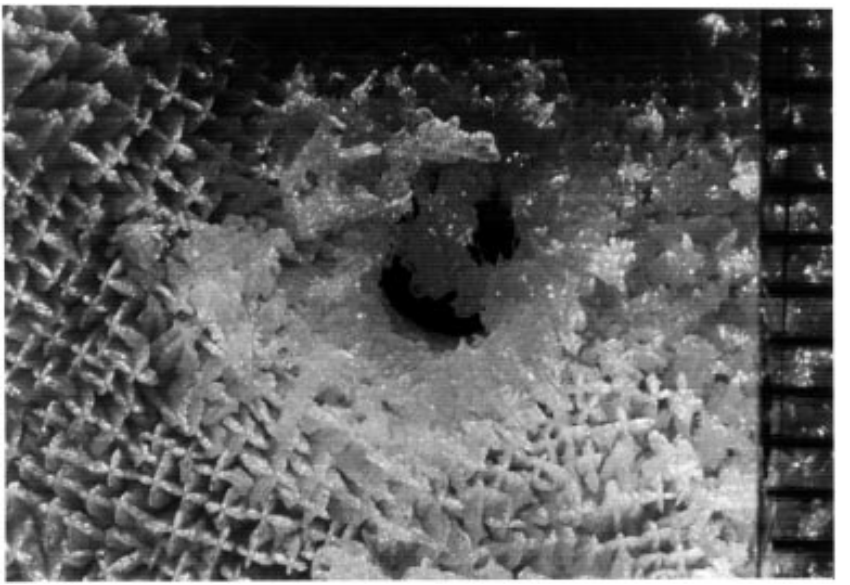

(b)

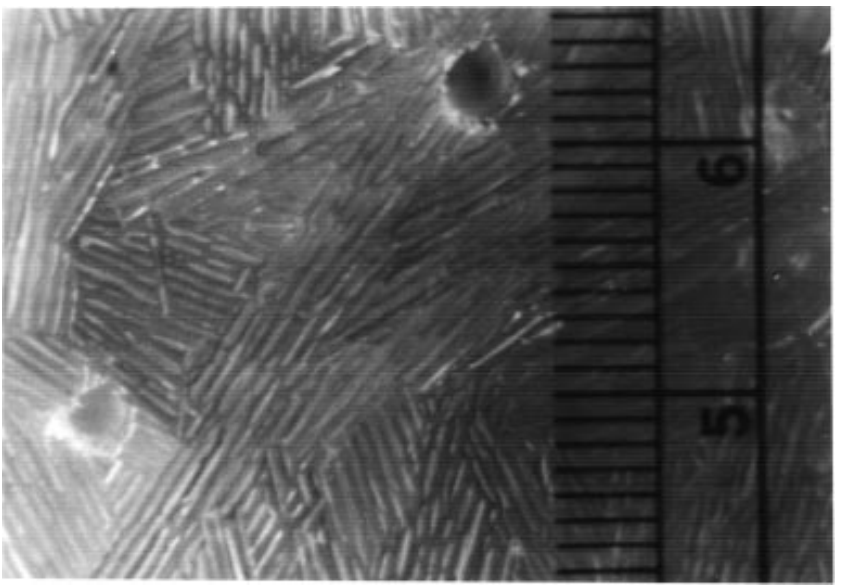

(c)

Figure 2 (*Continued*)

are discussed. Attention is focused in section 4 on convection that takes place entirely within the mushy layer. The significant dynamical interactions within the mushy layer are revealed by considering an asymptotic limit in which the mushy layer behaves as a passive porous medium and by systematically reintroducing terms into the equations. In this way, we shall review and place in context the various studies of linear and weakly nonlinear convection within mushy layers. The nonlinear studies reveal how the convective flow becomes focused into narrow regions of upflow that eventually become chimneys. In section 5, analyses of fully-developed chimneys are described, which have the aim of determining the overall fluxes from a convecting mushy layer. The experimental evidence for and against chimneys is discussed in section 6 along with suggestions for why chimneys may not form in nonideal mushy layers. The article concludes with a brief discussion of some of the applications of the theory of natural convection in mushy layers.

2. THE IDEAL MUSHY LAYER

Mathematical descriptions of mushy layers date back to metallurgical papers by Flemings & Nereo (1967), Mehrabian et al (1970) and Fujii et al (1979). These early studies aimed principally to relate measurements that could be made readily during casting, such as the temperature, to properties of the solidified product, such as the distribution of bulk composition. It is only in the last decade or so that equations have been formulated and solved in order to make predictions *ab initio* of solidification processes involving convection in mushy layers. All such mathematical models have as independent variables local mean properties of the mushy layer: mean temperature; mean concentration; and mean solid fraction. In all cases, the mean is taken (either formally or implicitly) over "infinitesimal" regions of the mushy layer that nevertheless contain representative distributions of liquid and solid phases. There are many assumptions made in taking such averages which are discussed in detail in the articles referenced below.

Different approaches to the formulation of governing equations have been taken by different authors. Conservation equations derived at the continuum level, with averaging implicit in their derivation, have been formulated by Fowler (1985) and Worster (1986) and reviewed by Worster (1992a). Still at the continuum level but using the formalism of thermodynamics, Hills et al (1983) based a derivation of governing equations on diffusive mixture theory. On the other hand, Emms (1993) has carried out an explicit averaging of governing equations for each phase. All of these models are expressed in terms of the primitive variables of temperature and concentration. An alternative approach is to replace temperature by enthalpy as a primary dependent variable,

which allows a single set of equations to describe both liquid and mushy regions. Equations of this sort have been derived, with explicit averaging, by Ni & Beckermann (1991) among others. They offer some computational advantages for full-scale numerical modeling but have been less used in analytical studies.

A fundamental distinction between the various formulations of mushy-layer equations is between those that employ mass-averaged variables and those that employ volume-averaged variables. When employing mass averaging it is usual to describe flow in terms of the barycentric velocity: the velocity of the local center of mass of the two phase medium. This has a natural interpretation in describing diffusively mixed fluid phases but is much less appropriate when one of the phases (here the solid matrix) is stationary. The flow through a mushy layer is better described by the local volume flux of liquid per unit area, or Darcy velocity (Phillips 1991).

The following equations define, at least for the purposes of this article, an ideal mushy layer. They encapsulate the essential physical interactions involved in all the formulations mentioned above. They are capable of describing all phenomena that have so far been determined theoretically. And they have the advantage of being simple and notationally familiar in the context of convective fluid dynamics. Their derivation (in a slightly more general form) can be found in Worster (1992a).

The flow through an ideal mushy layer is described by Darcy's equation

$$\mu \mathbf{u} = \Pi^*(-\nabla p + \rho \mathbf{g}), \tag{1}$$

which is the simplest description of flow through a porous medium. Here $\mathbf{u}$ is the Darcy velocity, p is the dynamic pressure, μ is the dynamic viscosity of the liquid and $\mathbf{g}$ is the acceleration due to gravity. The permeability $\Pi^*(\chi)$ is a function of the local liquid volume fraction $\chi = 1 - \phi$, where ϕ is the local volume fraction of solid. The density of the liquid is expressed as a linear function,

$$\rho = \rho_0[1 - \alpha^*(T - T_0) + \beta^*(C - C_0)], \tag{2}$$

of its concentration C and the temperature T, where ρ_0, T_0 and C_0 are reference values, and α^* and β^* are expansion coefficients for heat and salt, respectively. The interior of an ideal mushy layer is assumed to be in local thermodynamic equilibrium so that the temperature and the concentration of the liquid are coupled by the linear liquidus relationship (graphed in Figure 3)

$$T = T_L(C) \equiv T_E + \Gamma(C - C_E), \tag{3}$$

where Γ is the constant slope of the liquidus. The equation of state (2) thus

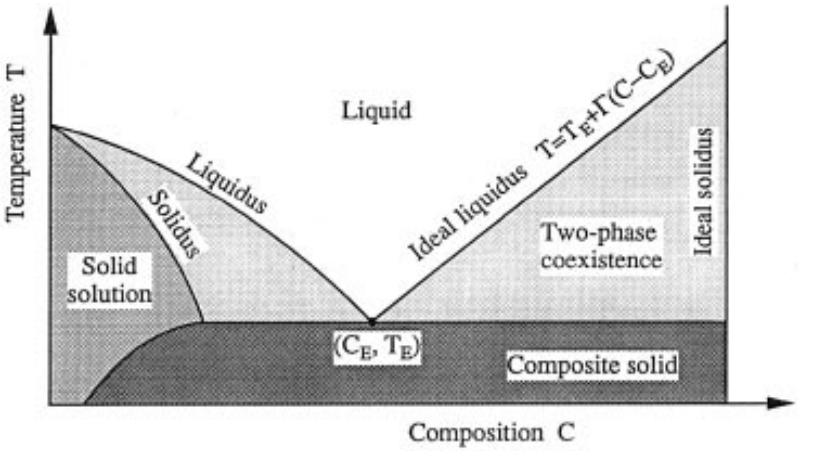

Figure 3 The equilibrium phase diagram of a typical eutectic binary alloy. The shaded regions show what phases exist in equilibrium in a sample of given bulk composition C and uniform temperature T. When the temperature is above the liquidus curve, the sample is completely liquid. In the region between the liquidus and the solidus, solid and liquid coexist in equilibrium, with the composition of the liquid phase equal to the liquidus concentration and the composition of the solid phase equal to the solidus concentration at the given temperature. This is the state in the interior of an ideal mushy layer. In general, the solid phase is a "solid solution" of the two components of the alloy: molecules of component B sit in a lattice of mostly A molecules (for example). In many cases the lattice parameters are such that solid solutions are not possible and the solid formed is almost pure, as shown on the right of the diagram. Below the eutectic temperature T_E, a composite solid forms composed of crystals of both of the end members of the alloy. In an ideal mushy layer, the liquidus is taken to be linear, as shown on the right.

adopts the simpler form

$$\rho = \rho_0[1 + \beta(C - C_0)], \tag{4}$$

where $\beta = \beta^* - \alpha^*\Gamma$.

Conservation of mass is expressed by the equation

$$\nabla \cdot \mathbf{u} = -\frac{\rho_s - \rho}{\rho}\frac{\partial \phi}{\partial t}, \tag{5}$$

where ρ_s is the density of the solid phase, and the Boussinesq approximation is invoked so that the density is constant except insofar as it modifies the buoyancy of the fluid. Equation 5 shows that the velocity field in a mushy layer is generally nonsolenoidal. The expansion or contraction that occurs on solidification of a liquid drives a flow in the absence of any external force, which can be significant in effecting global redistribution of solute (macro-segregation) in a casting (Petersen 1987, Schneider & Beckermann 1992, Chiareli et al 1994).

The flow can in principle also lead to instabilities that would result in lateral inhomogeneities developing during casting (Chiareli & Worster 1995) by a mechanism akin to the acid-etching instability in porous rocks (Chadam et al 1986, Sherwood 1987, Hinch & Bhatt 1990), though it seems unlikely that the criteria for instability will be met in practice. Here I restrict the definition of the ideal mushy layer by setting $\rho_s = \rho$ so that $\nabla \cdot \mathbf{u} = 0$.

Conservation of heat is described by the advection-diffusion equation

$$\left(\frac{\partial T}{\partial t} + \mathbf{u} \cdot \nabla T\right) = \kappa \nabla^2 T + \frac{L}{C_p}\frac{\partial \phi}{\partial t}, \tag{6}$$

where κ is the thermal diffusivity, C_p is the specific heat capacity and L is the latent heat per unit mass. The final term of this equation represents a heat source, which is due to the latent heat released as the melt solidifies within the interstices of the mushy layer. It provides an important coupling with the equation expressing conservation of solute

$$(1-\phi)\frac{\partial C}{\partial t} + \mathbf{u} \cdot \nabla C = (C - C_s)\frac{\partial \phi}{\partial t}, \tag{7}$$

where C_s is the composition of the solid phase. Diffusion of solute is neglected in an ideal mushy layer. This is justified on the grounds that the local concentration is tied to the temperature via the liquidus relationship and that in all systems of interest heat diffuses much faster than solute.

In principle, the solid fraction ϕ evolves in a way determined by interstitial gradients of heat and solute and by the specific surface area of internal phase boundaries. In an ideal mushy layer such interstitial gradients do not exist. Rather it is assumed that the specific surface area is sufficiently large to allow instantaneous relaxation of the solid fraction to achieve the equilibrium state described by Equation 3.

It is important to the fluid dynamics of mushy layers that they exist in a solidifying system so that the phase boundaries are continuously evolving. For example, in a continuous casting process phase boundaries advance at a constant rate, and during growth from a fixed, cooled boundary the phase boundaries advance proportional to the square root of time in the absence of convection. This makes convection in a mushy layer qualitatively different from convection in a Bénard cell that is stationary in a laboratory frame of reference. This inherent state of being nonstationary is most easily analyzed by considering systems that are solidifying at a constant rate V, as shown in Figure 4. Given this geometry, we can produce a set of dimensionless equations by scaling velocities with V, lengths with κ/V, time with κ/V^2 and by writing

$$\theta = \frac{T - T_E}{\Delta T} = \frac{C - C_E}{\Delta C}, \tag{8}$$

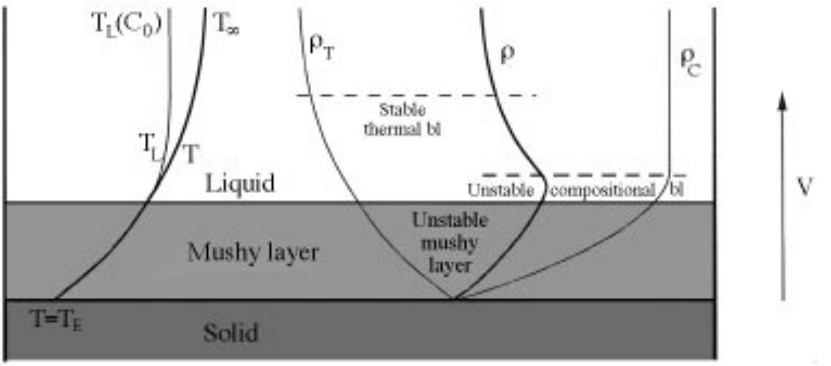

Figure 4 A schematic diagram of an alloy solidifying at a prescribed constant rate V. The alloy is completely solid where the temperature is below the eutectic temperature T_E. The profiles on the left show the temperature field T and the local liquidus temperature $T_L(C)$ in the nonconvecting state. These give rise to the density fields ρ_T and ρ_C, respectively, as shown in the diagram. The total density ρ is unstably stratified in the mushy layer and in a narrow boundary layer just above the mush–liquid interface. The thermal field creates a stable stratification throughout most of the liquid region.

where $\Delta T = T_L(C_0) - T_E = \Gamma \Delta C$, and T_E and C_E are the eutectic temperature and composition.

The full set of dimensionless equations describing the interior of an ideal mushy layer is then

$$\frac{\partial \theta}{\partial \tau} + \mathbf{u} \cdot \nabla \theta = \nabla^2 \theta + S \frac{\partial \phi}{\partial \tau} \tag{9}$$

$$\frac{\partial}{\partial \tau} [(1-\phi)(\theta - \mathcal{C})] = -\mathbf{u} \cdot \nabla \theta \tag{10}$$

$$\mathbf{u} = R_m \Pi(\chi) [-\nabla p - \theta \mathbf{k}] \tag{11}$$

$$\nabla \cdot \mathbf{u} = 0 \tag{12}$$

where $\frac{\partial}{\partial \tau} \equiv \frac{\partial}{\partial t} - \frac{\partial}{\partial z}$, $\mathbf{k}$ is a unit vector in the vertical direction and where the permeability Π has been made dimensionless with respect to a suitable reference value Π_0.

The dimensionless parameters governing convection in an ideal mushy layer are the Stefan number

$$S = \frac{L}{C_p \Delta T} \tag{13}$$

a compositional ratio

$$\mathcal{C} = \frac{C_s - C_E}{\Delta C} \tag{14}$$

and a Rayleigh number

$$R_m = \frac{\rho_0 \beta \Delta C g \Pi_0}{\mu V}. \tag{15}$$

The Stefan number measures the amount of latent heat that must be removed to effect the change of phase relative to the sensible heat that must be removed to cool the liquid from its liquidus to its solidus temperature. The ratio $\mathcal{C}$ gives the difference in composition between the liquid and solid phases relative to the compositional variation within the liquid phase. It plays a similar role for convection to that the Stefan number plays for heat. The Rayleigh number R_m is similar to that for convection in a porous medium and measures the buoyancy force, primarily due to compositional differences, relative to the viscous dissipation in the porous medium.

The term in square brackets in Equation 10, $(1 - \phi)(\theta - \mathcal{C})$, is the local bulk composition $\overline{C}$, averaged over both solid and liquid phases. Therefore, Equation 10 expresses the fact that bulk redistribution of solute in a mushy layer only occurs as a result of fluid transport.

The dynamics of the mushy layer are influenced by the fluid flow and heat transfer in the liquid region above it. These are described by the usual equations of convective fluid mechanics. We do not dwell on the dynamics of the liquid region here except to note that the coupling between the liquid and mushy regions depends principally on two further dimensionless parameters: the dimensionless far-field temperature

$$\theta_\infty = \frac{T_\infty - T_E}{\Delta T} \tag{16}$$

and a mobility ratio

$$\mathcal{H} = \frac{(\kappa / V)^2}{\Pi_0}. \tag{17}$$

The far-field temperature affects the depth of the mushy layer by influencing the heat flux transferred from the liquid region. For example, in the steady, nonconvecting state, it has been shown by Fowler (1985) and by Worster (1991) that the dimensionless depth of the mushy layer $\delta \sim 1/\theta_\infty$ when $\theta_\infty \gg 1$. The mobility ratio $\mathcal{H}$ is proportional to the square of the ratio of the depth of the mushy layer to the spacing between dendrites. It is therefore typically very large, in which case the dynamical influence of the liquid region reduces to a condition of constant pressure applied to the mush–liquid interface (Fowler 1985).

Equations 9–12 constitute a definition of an ideal mushy layer. They encapsulate the major known physical interactions that determine the evolution of mushy layers. Minor extensions to these equations, allowing for the solid

and liquid phases to have different physical and thermodynamic properties, can readily be made and are incorporated in the more general description given by Worster (1992a). Such extensions are necessary if accurate quantitative predictions are to be made but do not qualitatively affect the phenomenology of the mushy layer.

3. LINEAR CONVECTIVE INSTABILITY

3.1 *The Full System*

There are steady, nonconvecting solutions to Equation 9–12, coupled with the equations for diffusion of heat and solute in the liquid region (Hills et al 1983, Fowler 1985, Worster 1991). They are characterized by temperature and concentration fields that give rise to the density profiles sketched in Figure 4 (Worster 1992b). It is apparent that there is an unstable density difference across the mushy layer and a much smaller, unstable density difference across a compositional boundary layer in the liquid just above the mush–liquid interface. Although the dominant forcing is within the mushy layer, the liquid in the compositional boundary layer is much more mobile. In fact the Rayleigh number characterizing the boundary layer R_l scales with $\epsilon^3 \mathcal{H} R_m$, where $\epsilon = D/\kappa \ll 1$ (D is the diffusivity of salt) and $\mathcal{H} \gg 1$ is the mobility ratio described earlier (Tait & Jaupart 1989, Worster 1992b). The small factor ϵ^3 reflects the thinness of the boundary layer relative to the depth of the mushy layer as well as the smallness of the density contrast across it relative to that across the mushy layer. It is countered by the greater mobility of the liquid region, characterized by $\mathcal{H}$.

A detailed linear stability analysis (Worster 1992b) revealed that the marginal stability curve for direct (nonoscillatory) modes of convection is typically bimodal, as illustrated in Figure 5. There is a "boundary-layer mode" of convection on length scales characteristic of the thickness of the compositional boundary layer and a "mushy-layer mode" on longer length scales characteristic of the depth of the mushy layer. Broadly speaking, onset of the boundary-layer mode is determined by the magnitude of R_l, while onset of the mushy-layer mode is determined by R_m. Figure 5 was produced with $R_l \approx 1.56 R_m$ and we see that the two modes are triggered almost simultaneously.

It is difficult to measure the permeability of the mushy layer, though sensible estimates can be made (e.g. Tait & Jaupart 1992, Ganesan et al 1992). Using these, it can be determined that R_m and R_l have comparable magnitudes (within the uncertainties of the estimates) in typical laboratory experiments using aqueous solutions of ammonium chloride. However, there is experimental evidence that typically $R_l > R_m$ since it is usual to see fine-scale convection arising from the neighborhood of the mush–liquid interface (in the form of double-diffusive

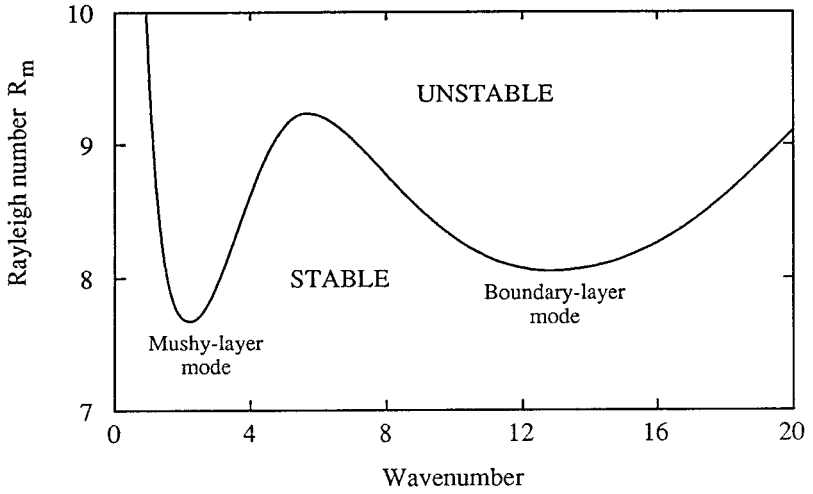

Figure 5 The marginal stability curve corresponding to the compositional density field ρ_C shown in Figure 4. The curve has two minima corresponding to two modes of steady convection that can occur. There is a boundary-layer mode at large wavenumber (small wavelength) and a mushy-layer mode at a smaller wavenumber.

fingers) well before any discernable fluid motion in the mushy layer (Tait & Jaupart 1989, Chen & Chen 1991, Chen 1995) or the appearance of chimneys.

The linear stability analysis was extended by Chen et al (1994) to include the possibility of oscillatory onset. They found that the two direct modes can separate by means of an oscillatory connection as the stable thermal buoyancy increases. With hindsight, such oscillations might have been anticipated on the grounds that the region of stable buoyancy in the liquid above the mushy layer can support internal gravity waves. The results of Chen et al (1994) suggest further that the oscillations they found arise from a linear interaction between a one-cell mode and a two-cell (vertically stacked) mode in the liquid region. It is also possible that oscillatory convection in a mushy layer has an entirely different origin, as we shall see below. Oscillatory convection was in fact first discovered by Nandapurkar et al (1989) but since their numerical analysis was conducted using particular dimensional parameters and covered only a fraction of the marginal curve, it was difficult to ascertain the cause of the oscillations.

Given that, experimentally, double-diffusive fingers are well developed in the liquid region before the genesis of chimneys, it is appropriate to ask what influence such convection has on the onset of the mushy-layer mode. This question

was answered by Emms & Fowler (1994), who showed that the fingers produce, in the mean, an enhancement of the thermal diffusivity of the liquid. However, the effect is very small and for practical purposes can be ignored.

All indications to date are that the experimental observations relating to chimney formation in mushy layers are entirely consistent with the nonlinear development of the nonoscillatory, mushy-layer mode of convection. For this reason, it has proved expedient to consider restrictions of the mathematical model that eliminate any interaction between the liquid and mushy regions.

3.2 *A Restricted Model*

The full system of mushy layer and overlying liquid region is mathematically very cumbersome. The equations are fifth-order in the mushy layer, eighth-order in the semi-infinite liquid region, and there is a free interface between the two domains. This makes even a linear-stability analysis challenging and a nonlinear analysis of the full equations presently inconceivable. For this reason, restrictions to the model have been sought that allow greater progress while not compromising the essential physical interactions intrinsic to the evolution of the mushy layer.

In this section, I present equations that are simply illustrative of the physical interactions retained in each restricted study. The actual equations solved in each case were much more detailed and were formally derived using appropriate asymptotics from the full equations.

Fowler (1985) was the first to suggest reducing the governing equations by taking asymptotic limits of the controlling dimensionless parameters. He introduced a "near-eutectic" approximation in which the initial (or far-field) concentration C_0 is assumed to be very close to the eutectic concentration C_E. Using the notation of Section 2, his approximation is equivalent to taking $\mathcal{C} \to \infty$ and $\theta_\infty \to \infty$ with $\theta_\infty/\mathcal{C} = O(1)$. This has recently been shown to be a singular limit for the full time-dependent equations (Anderson & Worster 1995) but it gives the correct leading-order behavior both for the state with no fluid motion and for marginal linear stability of that state.

The near-eutectic limit has the effect of making the dimensionless thickness of the mushy layer $\delta \ll 1$ and the solid fraction $\phi \ll 1$: specifically, $\delta = O(\theta_\infty^{-1})$ and $\phi = O(\mathcal{C}^{-1})$. Since $\phi \ll 1$ in this limit, it is important to adopt a permeability function $\Pi(\chi)$ that remains bounded as $\phi \to 0$, $\chi \to 1$. The most important consequence of the near-eutectic approximation is that one recovers exactly the classical problem of convection in a nonreacting porous layer (Horton & Rogers 1945, Lapwood 1948, Palm et al 1972). The solute-conservation equation (Equation 10) decouples from the other equations, the linearized versions of which describe the onset of convection in a passive porous

medium. This can be represented by

$$\dot{W} = (R - 1)W, \tag{18}$$

where W represents a (vertical) velocity which grows exponentially when the Rayleigh number R exceeds a critical value, here set equal to unity. The solute-conservation equation then simply determines how the solid fraction evolves in response to the velocity field, and is essentially described by

$$\dot{\phi} = -\mathcal{C}^{-1}W. \tag{19}$$

Where there is upflow ($W > 0$), the solid fraction decreases as a consequence of cold but dilute fluid dissolving the crystals around which it flows. A parcel of fluid raised upwards finds itself colder and fresher than its new surroundings. It warms quickly by thermal diffusion but retains its composition since the solutal diffusivity is small (equal to zero in an ideal mushy layer) relative to the thermal diffusivity. This much is true even in a non-reacting porous medium. In a mushy layer, however, the parcel of fluid, being now of similar temperature but lower concentration than its surroundings, is undersaturated and partly dissolves the solid phase until its concentration is equilibrated with the local liquidus.

This is a fundamental property of flow in mushy layers—that dissolution occurs where there is a component of flow parallel to the local temperature gradient (from cold to warm). This mechanism for producing channels within mushy layers has long been known to metallurgists (Flemings 1974), who developed the criterion, elucidated by Fowler (1985),

$$(\mathbf{u} - \mathbf{V}) \cdot \nabla T > 0 \tag{20}$$

for when channels will form, where $\mathbf{V}$ is the solidification rate.

The near-eutectic approximation, as described so far, contains none of the coupled interactions between solidification and flow that distinguish convection in mushy layers from classical fluid convection and make its study so fascinating. However, it makes an excellent foundation, being a limit that is well understood and to which other effects can be added as small perturbations.

A physical process intrinsic to mushy layers is the release of latent heat as the solid fraction increases. This can be reintroduced into the near-eutectic equations by taking $S = O(\mathcal{C})$, instead of $S = O(1)$ as before. The essential effect of this distinguished limit, introduced by Emms & Fowler (1994), is illustrated by a modified version of Equation 18:

$$\dot{W} = (R - 1)W - S\dot{\phi}. \tag{21}$$

The added term needs some explanation. Given that the interior of the mushy layer is constrained by the liquidus relationship, it adjusts to phase changes as

follows. During solidification, the release of latent heat, proportional to $\dot{\phi}$, tends to warm the mushy layer. The liquidus constraint then requires the interstitial liquid to become saltier and, therefore, heavier, which tends to retard growth of the vertical velocity.

The release of latent heat would appear to couple the convection, represented by Equation 21, to the evolution of the solid fraction, represented by Equation 19. However, these equations are readily combined to give the uncoupled convection problem

$$\dot{W} = (R - 1 + S/\mathcal{C})W, \tag{22}$$

derived in full by Emms & Fowler (1994). This equation illustrates the initially surprising result that linear disturbances are more unstable when the latent heat is large (Worster 1992b). When the Stefan number is large, a given thermal perturbation can dissolve less of the solid phase and hence there is less heavy solute introduced into the liquid.

Another surprise comes from considering more closely the structure of the solute-conservation equation (Equation 10) which is better modeled by

$$\dot{\phi} + V(\phi - \phi_e) = -\mathcal{C}^{-1}W, \tag{23}$$

than by Equation 19. The additional term on the left-hand side, proportional to V, reintroduces the fact that the system is continuously being solidified. Therefore, in the absence of flow ($W = 0$), the system relaxes to an equilibrium state $\phi = \phi_e$. This occurs at a rate proportional to the background solidification rate V. The additional term, though apparently causing a decay of perturbations to the solid fraction, can actually destabilize the system to an oscillatory mode of convection that can set in before the steady mode found previously. This can be seen by combining Equations 21 and 23 to give

$$\begin{pmatrix} \dot{W} \\ \dot{\phi}' \end{pmatrix} = \begin{pmatrix} R - 1 + S/\mathcal{C} & SV \\ -\mathcal{C}^{-1} & -V \end{pmatrix} \begin{pmatrix} W \\ \phi' \end{pmatrix}, \tag{24}$$

where $\phi' = \phi - \phi_e$. The possibility of oscillations is evident from the fact that the off-diagonal terms have opposite signs. The characteristics of the eigensolutions of Equation 24 are shown in Figure 6, the topology of which is preserved by the full system of Equations 9–12 (Anderson & Worster 1996). The linear oscillatory mode is a consequence of intricate interactions between convection and solidification in a mushy layer and has no analogue in simple Bénard convection. These oscillations clearly have nothing to do with internal waves in the melt but are intrinsic to the internal dynamics of the mushy layer.

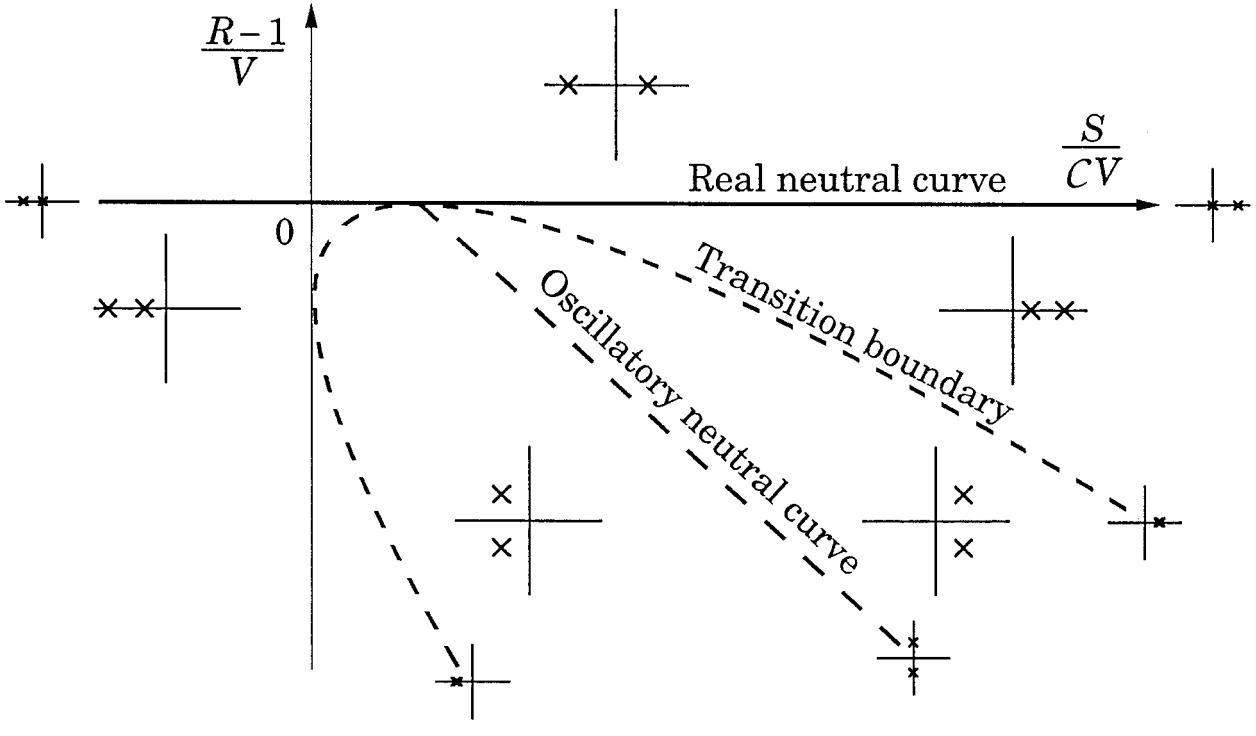

Figure 6 The different linear mushy-layer modes of convection that can occur within an ideal mushy layer. The larger inset graphs show the location of the eigenvalues of Equations 24 in the complex plane corresponding to states (starting at the top and going clockwise) in which there is one stable and one unstable steady mode, two unstable steady modes, two unstable oscillatory modes, two stable oscillatory modes, and two stable steady modes. The smaller inset graphs show the transitional states. Although the diagram was produced from the illustrative model Equations 24, its topology is preserved by the full equations governing an ideal mushy layer.

4. NONLINEAR CONVECTION

As we have seen, there are interesting novel phenomena associated with linear convection in mushy layers. Some of these are indicative of the mechanisms underlying chimney formation, but the focusing of the convective flow into narrow vertical regions of upflow is fundamentally a nonlinear phenomenon. In particular, the linear analyses cannot capture the effect of changing solid fraction on the permeablity to flow, which provides a positive nonlinear feedback for convection.

Amberg & Homsy (1993) were the first to analyze such nonlinear mechanisms with a small, finite-amplitude analysis of convection in a mushy layer. They employed the near-eutectic approximation and further restricted their analysis by imagining a (co-moving) rigid barrier to separate the mush from the liquid region. The essential physics underlying their analysis is illustrated by the equations

$$\dot{W} = [R(\phi) - 1]W \tag{25}$$

and

$$\dot{\phi} = -\mathcal{C}^{-1}W. \tag{26}$$

Of course, the equations actually solved were much more complex and the solution involved a double expansion in $\delta \ll 1$ and $\epsilon \ll 1$ in the distinguished limit $\delta \sim \epsilon$, where δ is the dimensionless depth of the mushy layer and ϵ is the amplitude of the perturbations. They analyzed, separately, weakly nonlinear steady states in the form of 2-D rolls and of hexagons.

An important parameter determining the nonlinear evolution of convection in a mushy layer is the sensitivity of its permeability to changes in the solid fraction, $\mathcal{P} = -\frac{1}{\Pi}\frac{d\Pi}{d\phi}$, which is constant in the near-eutectic limit. It is related to $R'(\phi)$ in the illustrative Equation 25. In the near-eutectic approximation, the permeability is given by

$$\Pi^* \sim \Pi_0(1 - \mathcal{P}\phi + \cdots). \tag{27}$$

Amberg & Homsy (1993) found that 2-D rolls bifurcate supercritically when $\mathcal{P}$ is small but bifurcate subcritically when $\mathcal{P} > 0.226\delta\mathcal{C}$. They found further that hexagons bifurcate linearly, the backwards branch corresponding to hexagons with upflow at their centers.

The only experimental study relating to this result is that by Tait et al (1992), who cooled and solidified solutions of ammonium chloride from below very slowly so that they could observe the onset of convection. The most striking observation was of vertical, sheet-like chimneys forming the sides of a roughly polygonal array. A statistical analysis of the numbers of nodes in the array and

the lengths of sides of the polygons gave numbers that, of all the possible tesselating plan forms, were closest to hexagons. The flow was downwards at the centers of the hexagons and upwards along their edges, where the crystals were dissolved to form linear chimneys. The nodes where edges met eventually became the familiar cylindrical chimneys, while further crystallization filled the edges.

The observation of hexagons with downflow at their centers is at variance with the results of Amberg & Homsy (1993), since one would expect the conditions relating to the backward branch of the bifurcation diagram to be observed first. Their analysis was extended recently by Anderson & Worster (1995) in two ways. First, they relaxed the condition $\delta \sim \epsilon$ and instead considered the double limit $\lim_{\delta\to 0}\lim_{\epsilon\to 0}$, noting that this is quite distinct from $\lim_{\epsilon\to 0}\lim_{\delta\to 0}$, which is singular. This allowed them to include many more nonlinear effects in addition to the variation of permeability with solid fraction. Second, they formally set $\mathcal{P} = O(\epsilon)$, which makes the linear branch corresponding to hexagons almost vertical, allowing higher-order terms to be included in the analysis and allowing the interactions between rolls and hexagons to be studied. It was found that both stable up-flowing and stable down-flowing hexagons are possible depending on the dimensionless parameters of the system (Figure 7). While the analysis still cannot be compared directly to the experimental results, it illustrates how many different factors contribute to the planform of convection in mushy layers. More importantly, this study revealed the parametric dependence of the global critical Rayleigh number R_g, below which the system is completely stable to disturbances of arbitrary amplitude.

A major shortcoming of the nonlinear analyses described above is the use of the boundary condition of no vertical flow through the mush–liquid interface. This was employed expediently to allow analytical progress to be made, but a more appropriate condition would be one of constant pressure. It is likely that a numerical study will be needed to study this case.

As one moves along the nonlinear branch of the bifurcation diagram (Figure 7) to larger amplitudes, the flow evolves from the sinusoidal profile of the linear normal mode to a profile in which the upflow is focused into narrow vertical regions separated by broader regions of downflow (Figure 8). Eventually one reaches a state in which the solid fraction is negative immediately below the top of the region of upflow: a chimney is born at the mush–liquid interface and "grows downwards" into the mushy layer. Similar behavior has been seen in full-scale numerical simulations by Fellicelli et al (1991), though the calculations were not well resolved. The fact that chimneys grow from the top down appears to give support to the idea, mooted by Sample & Hellawell (1984), that chimneys form in response to the convective flow in the liquid region above the mushy layer. However, as has been noted by many authors, the apparent growth

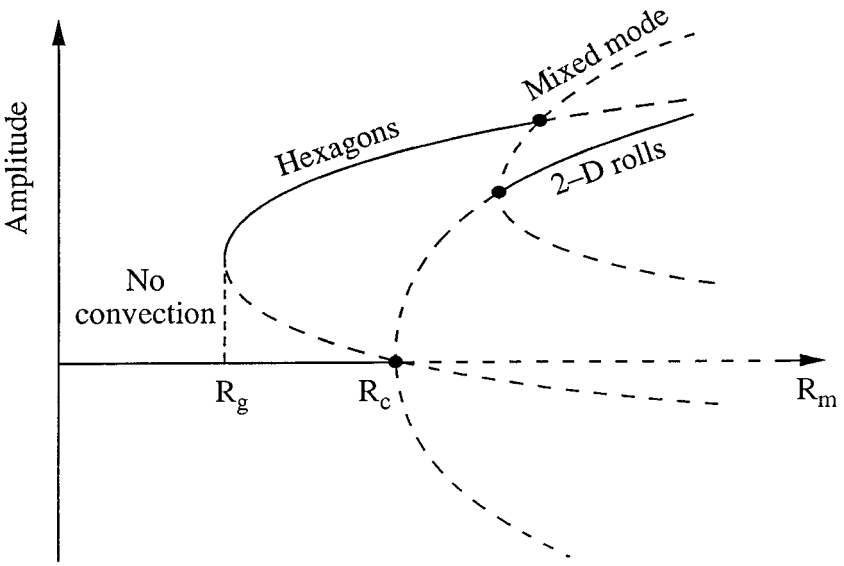

Figure 7 The bifurcation diagram for weakly nonlinear convection in a mushy layer, showing the interaction between 2-D rolls and hexagons. The figure is drawn for the case that up-flowing hexagons are stable. For other values of the governing parameters the figure becomes reflected in the ordinate axis so that down-flowing hexagons are stable. Below the minimum Rayleigh number R_g the mushy layer is completely stable to disturbances of arbitrary amplitude. Solid curves indicate stable steady states, while dashed curves indicate unstable steady states.

from the top down is simply a consequence of the fact that the solid fraction is smallest and the vertical velocity is largest at the top of the mushy layer. The mechanism producing chimneys is internal to the mushy layer itself, though convective motions above the mushy layer may help to trigger the subcritical convection within it.

5. FULLY DEVELOPED CHIMNEYS

Once a region of the mathematical mushy layer attains a negative solid fraction it must be replaced by liquid, whose motion is governed by the full Navier-Stokes equations. This significantly increases the difficulty of calculating large-amplitude convecting states.

An alternative approach is to try to describe, mathematically, convective states in which the chimneys are fully developed. Historically speaking, this is perhaps the beginning of the story of attempts to calculate flows in mushy layers. The first analytical treatment of flow in a mushy layer was presented by Roberts & Loper (1983). They considered flow in an annular mushy region, with the

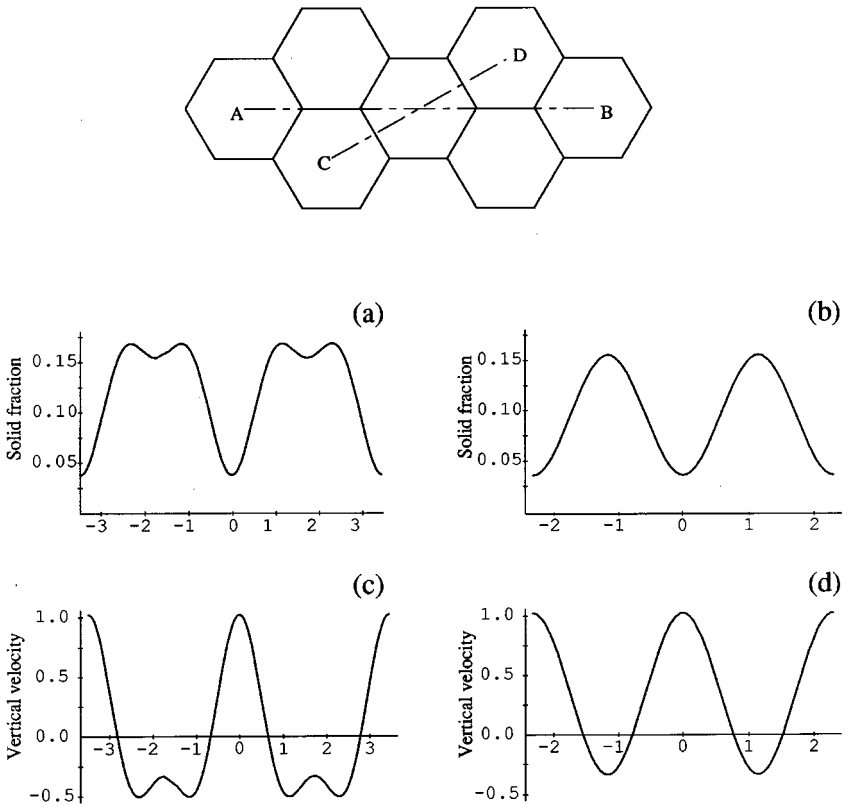

Figure 8 The solid fraction and vertical velocity as functions of horizontal distance in a nonlinear convecting state with hexagonal planform. Figures (*a*) and (*b*) correspond to the section AB and figures (*c*) and (*d*) correspond to the section CD in the hexagonal planform shown above. There is upflow in the center of each hexagon, which leads to dissolution of the solid fraction there. The parameter values used were $\delta = 0.3$, $\mathcal{C} = S = 2$ and $\epsilon = 0.005$. The figure was produced by DM Anderson, based on the study by Anderson & Worster (1995).

core of the annulus being a chimney. They developed a consistent framework in which fluid flowed from the liquid region above the mushy layer down and inwards toward the chimney and then flowed up through the chimney driven by buoyancy forces within the chimney and the pressure gradient along the wall of the chimney. This framework was adopted by Worster (1991), who analyzed the asymptotic limit of large Rayleigh number. His study suggested that the solid fraction at first increases toward the chimney, owing to the additional cooling provided by the flow of cold liquid up the chimney, before decreasing to zero

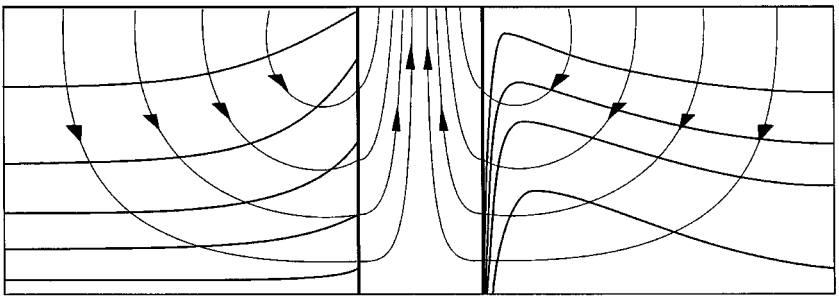

Figure 9 The streamlines once a chimney has formed in a two-dimensional ideal mushy layer are shown with thin lines, with arrows indicating the direction of flow. Superimposed on the left are isotherms and on the right are contours of solid fraction. The chimney (central portion) is assumed to have straight-sided walls. The scale of the chimney shown in the figure is arbitrary. The ratio of the actual width of the chimney to the width of the convection cell depends on the dimensionless parameter $\mathcal{H}$. The flow in the chimney was calculated analytically using an approximate Polhausen method, while the flow in the mushy layer was calculated numerically. Although the top of the mushy layer was kept flat and horizontal in the calculation, the shape of the solid-fraction contours is indicative of the shape of the mush-liquid interface. The calculations were made recently by TP Schulze.

very close to the chimney wall, owing to internal dissolution. This picture has recently been confirmed by direct numerical calculation (Figure 9).

Although the asymptotic analysis enabled the width of a single chimney and the strength of the flow through it to be determined, the overall heat and salt fluxes exchanged between the mushy layer and the liquid region depend also on the areal number density of chimneys $\mathcal{N}$. A theoretical prediction of $\mathcal{N}$ has yet to be made, which is perhaps now the major obstacle preventing simple completely predictive models of fully convecting systems including mushy layers to be developed.

Some important general results have, nevertheless, been obtained by prescribing a fixed value for $\mathcal{N}$. Among these is the fact that, once chimneys are fully developed, the temperature and concentration of the liquid region evolve towards less saturated conditions (Worster 1990). This is in contrast to the effect of convection from the mush–liquid interface (the boundary-layer mode), which tends to cause the liquid region to become supercooled (Kerr et al 1990). It has also been possible to calculate, as a function of $\mathcal{N}$, the effect on the horizontally averaged solid fraction of convection through chimneys in the mushy layer. Such convection increases the solid fraction significantly. Worster (1991), for example, showed that the solid fraction could become equal to unity at the base of the mushy layer and hence that the composition of the solid below the eutectic front could become equal to that of the pure salt. However, his calculation neglected the decrease of the permeability as the solid fraction

increases, which inhibits the removal of residual liquid from the interstices. This effect is currently being investigated in the context of the desalination of marine ice, described in Section 7, below.

6. WHY CHIMNEYS MAY NOT FORM

In the last few sections, I have summarized the theoretical studies of ideal mushy layers in a way that suggests that chimneys are an inevitable consequence of convection in mushy layers if only the Rayleigh number is large enough. All experimental studies of mushy layers have been transient ones in which cooling has been applied at a fixed boundary and the mushy layer has grown in depth away from the boundary. From what has been described so far, since the Rayleigh number increases with the depth of the mushy layer, one would reasonably expect the mushy layer to grow initially without convecting, then begin convecting once the depth achieves a certain value, and to produce chimneys once the depth achieves a certain greater value. This is precisely the sequence of events that is observed when aqueous solutions of ammonium chloride are cooled and solidified from below. However, in many similar experiments using various other salts no chimneys were ever observed (Huppert 1990).

One of the difficulties in determining the reason or reasons for the lack of chimneys in certain experiments was that there were so many gross differences between the various experiments, both chemically and physically. What was needed was a systematic and quantitative way of making a mushy layer progressively more nonideal.

Such a method was discovered by Huppert & Hallworth (1993). To aqueous solutions of ammonium chloride they added small quantities (up to 0.5 wt.%) of copper sulfate. It had been known for a long time that, as the concentration of copper sulfate added to aqueous ammonium chloride solutions increases, the crystals that form undergo various morphological phase transitions associated with exposing new crystallographic planes to the melt, and that the crystals become more faceted (Mellor 1981). These are microscopic effects. What Huppert & Hallworth (1993) discovered was the macroscopic phenomenon that the time until the first appearance of chimneys increased dramatically as the concentration of copper sulfate increased until, at a concentration of a little over 0.3 wt.% $CuSO_4$, no chimneys were observed at all.

Before describing possible reasons for this phenomenon in terms of nonideal effects, let us examine the possibilities for the nonappearance of chimneys based on the behavior of ideal mushy layers.

The simplest explanation is that, since the critical Rayleigh number depends on all the other dimensionless parameters of the system, such as S and $\mathcal{C}$, it was simply never attained in the experiments in which chimneys were not observed. Appealing as this is, by itself it is perhaps too simple to explain the results of

adding copper sulfate to solutions of ammonium chloride. The only way to change the critical Rayleigh number substantially is to change the steady-state solid fraction of the mushy layer. The small amounts of copper sulfate added have only a small effect on the equilibrium phase diagram and hence have little effect on the solid fraction.

Another possibility is a little more subtle. Along the nonlinear branch of the bifurcation diagram (Figure 7), chimneys can appear either on the lower (unstable) branch or on the upper (stable) branch depending on the values of the dimensionless parameters (Anderson & Worster 1995). In the former case, any triggering of convection leads inexorably to the appearance of chimneys. In the latter case, stable, finite-amplitude-convection states are possible with no chimneys. Such convection, by bringing more solute into the mushy layer, increases the bulk concentration of the layer and hence increases its solid fraction, retarding further amplification of the convection and delaying the formation of chimneys. This may be a significant or even the dominant reason why chimneys are not seen in many experiments, but seems unlikely to be sufficient to explain the dramatic consequences of small additions of copper sulfate to ammonium chloride solutions.

It is tempting to conclude from Huppert & Hallworth's experiments that, since copper sulfate alters the structure of the crystals, convection in mushy layers is very sensitive to the morphology of the solid phase. However, while there is some influence of morphology on the permeability, the latter is principally determined by the primary dendrite spacing, which does not change significantly.

However, the changed morphology, particularly the increasingly faceted appearance of the crystals, is indicative of greater levels of kinetic undercooling at the crystal–melt interface. This has been measured directly by Raz et al (1991). Kinetic undercooling is essentially the activation energy that is required for molecules to leave the liquid phase and become part of the solid. It manifests itself in the fact that the temperature at the interface of a growing crystal is less than the equilibrium freezing temperature (liquidus) by an amount that is a function of the growth rate of the crystal. At the mush–liquid interface there is an interfacial undercooling resulting from three effects: the attachment kinetics just mentioned; undercooling associated with the curvature of the dendrite tips; and constitutional undercooling owing to compositional depletion in the vicinity of the growing dendrites.

Kerr et al (1990) had shown how such interfacial undercooling just at the edge of a mushy layer, coupled with convection in the liquid region, can have profound consequences for the evolution of the liquid and the growth of the mushy layer. In 1994, Worster & Kerr applied this same idea to the experiments of Huppert & Hallworth. They measured the interfacial undercooling at the mush–liquid interface and determined an empirical relationship of the form

$$\dot{h} = \mathcal{G}(T_L - T_i)^2, \tag{28}$$

where $\dot{h}$ is the rate of advance of the interface, T_L is the liquidus temperature of the melt, T_i is the temperature of the interface, and $\mathcal{G}$ is a constant. This functional form is motivated by physical principles of local crystallization kinetics, which can depend on crystal orientation and the growth mechanism at the molecular level (Burton et al 1951). Worster & Kerr (1994) found that the coefficient $\mathcal{G}$ is a very strong function of the concentration of copper sulfate. They incorporated the measured values of the undercooling into a theoretical analysis of a growing mushy layer. They showed how the undercooling causes a strengthening of the boundary-layer mode of convection, which retards growth of the mushy layer, increases its solid fraction, and decreases the compositional contrast across it. These three effects combine to reduce the Rayleigh number of the mushy layer. It was shown in particular that, although it always increases initially, the Rayleigh number can ultimately decrease in time (Figure 10). It thus reaches a maximum value which can be less that that required for chimneys to form.

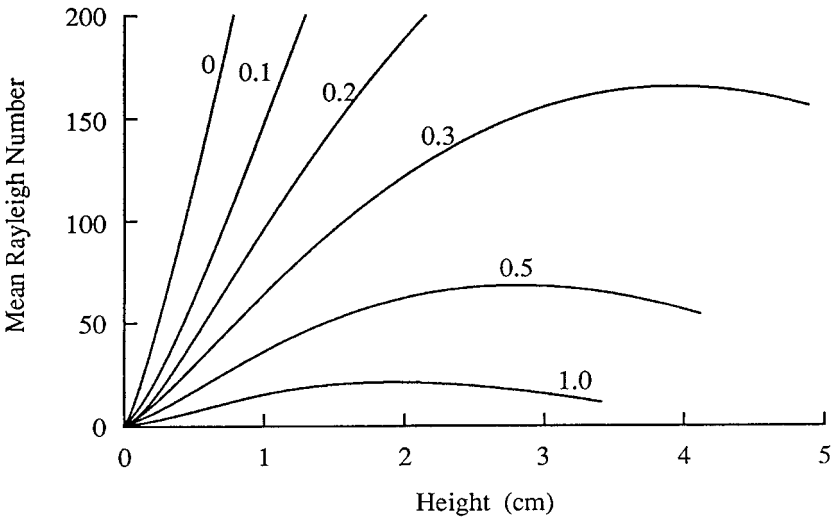

Figure 10 The calculated Rayleigh number in a stagnant mushy layer growing from a cooled lower boundary as a function of time. The liquid above the mushy layer is assumed to be convecting vigorously, driven by compositional buoyancy in the neighborhood of the mush–liquid interface. The convection coupled with dynamic interfacial undercooling causes the composition of the melt to evolve, retards growth of the mushy layer, and increases its solid fraction. These effects combine to reduce the Rayleigh number and can cause it ultimately to decrease, as shown. The numbers labeling the curves correspond to the concentration (wt.%) of copper sulfate with which an aqueous solution of ammonium chloride was contaminated. Increasing the contamination makes the mushy layer progressively less ideal. At a sufficiently high contamination the maximum Rayleigh number attained is less than that required for chimneys to form in the mushy layer.

An alternative explanation, suggested by S. Lipson in an appendix to Huppert & Hallworth (1993), is that the interstitial liquid may convect out of the mushy layer before becoming unsaturated sufficiently to dissolve any crystals. This requires disequilibrium in the interior of the mushy layer and hence a greater departure from the ideal mushy layer than does the explanation given by Worster & Kerr (1994). This suggestion has yet to be given quantitative substance, which awaits the development of a mathematical model of a nonideal mushy layer.

7. SOME APPLICATIONS

The study of mushy layers was introduced to the applied-mathematics community from metallurgy by some of those interested in the convective dynamics of the Earth's core and the geodynamo (Fearn et al 1981). The Earth's core consists of a solid inner core of iron growing from an outer core of molten iron contaminated by small amounts of lighter elements such as sulfur and oxygen. The conditions (pressure, temperature, concentration) are such that the inner core is potentially mushy throughout (Fearn et al 1981). As more iron solidifies onto the inner core, the molten outer core becomes enriched in the lighter elements and may therefore undergo compositional convection. As we have seen, such convection can lead to the formation of chimneys and focusing of the flow into narrow buoyant plumes. The structure of the convective elements can have a profound influence on their potential to generate or sustain a magnetic field (Moffat & Loper 1994). Recently the idea that convection in the mushy inner core leads to chimneys has been challenged by Bergman & Fearn (1994). They argue that the resistance to flow through the inner core is dominated by the magnetic field so that the nonlinear feedback associated with decreasing solid fraction increasing the permeability may be ineffectual in focusing the flow to form chimneys.

Mushy layers are also prevalent in solidifying magmas and one might anticipate that chimneys should be observed in igneous rocks. A significant difference between a solidifying magma and a directionally cast alloy is that many crystals in a magma grow in suspension and then settle to form a "cumulate pile". Though morphologically different from a dendritic mushy layer, continuing solidification of interstitial melt in a cumulate pile may generate similar convective flows within it (Kerr & Tait 1986, Tait & Kerr 1987). Such flows can become focused by the same mechanisms associated with dissolution that have been described here and either form chimneys or simply narrow vertical regions of slightly altered composition and microstructure. Such postcumulate processes in magma chambers have not yet received much attention, though some connections between the chimneys observed in mushy layers in laboratory experiments and geological field data have been made by Tait & Jaupart

(1992), who suggested, for example, that dunite pipes in the Bushveld intrusion (in South Africa) may be extinct chimneys.

Another form of cumulate pile occurs on the underside of Antarctic ice shelves. Melt water formed near the grounding line of an ice shelf flows up along the underside of the shelf in a buoyant plume (Jenkins & Bombosch 1995). As the plume rises, it experiences a fall in the surrounding hydrostatic pressure and can begin to solidify. Ice crystals are believed to accrete from the plume to the underside of the ice shelf to form a layer of "marine ice". The layer of ice crystals will initially have salt water in its interstices, and the bulk salinity of the layer will therefore be about 1 ppt. Yet the bulk salinity of marine ice recovered from drilling surveys has a salinity of only 0.05 ppt. One mechanism that could account for this desalination is the drainage of brine through chimneys that form during freezing of the interstices.

Such drainage is certainly evident during the formation of sea ice in polar seas (Eide & Martin 1975). Sea ice forms initially by the aggregation of frazil ice crystals in suspension (Martin 1981) but it quickly develops into a mushy layer with a rigid matrix of solid ice. In this and in the case of marine ice, cooling is from above, though in the case of marine ice the cooling is very weak. Strictly, therefore, these are dynamically different situations from that discussed above, in which cooling was from below. However, the internal dynamics of the mushy layer are similar but with the effective expansion coefficient redefined by $\beta = \beta^* + \alpha^*\Gamma$, since thermal and compositional buoyancy act in concert when cooling is from above. Recent experiments by JS Wettlaufer, HE Huppert and myself have shown that when a mushy layer of sea ice first begins to grow in open water, the rejected brine initially remains within its interstices. Only once the depth of the sea ice exceeds a critical value (depending on the surface temperature) does brine begin to drain into the underlying ocean (Figure 11). This is consistent with the ideas presented here that mushy layers remain stagnant until the Rayleigh number R_m exceeds a critical value.

Of course, one of the main applications of all this work remains the analysis of industrial casting processes. The longitudinal strength of turbine blades, for example, is significantly enhanced by solidifying them directionally. This is done by withdrawing the mold slowly and vertically downwards from the furnace so that crystals grow upwards from the base of the mold. The state of the art is to grow single-crystal turbine blades. The solid phase during solidification is still dendritic (similar in appearance to Figure 1), but all the dendrites originate from the same single crystal seed. Such regular alignment increases the permeability of the mushy layer and hence increases the potential for convection and the formation of chimneys. Solidified chimneys, called "freckles", are regions of altered composition and microstructure that seriously impair the strength of the cast product. Current industrial practice is simply to

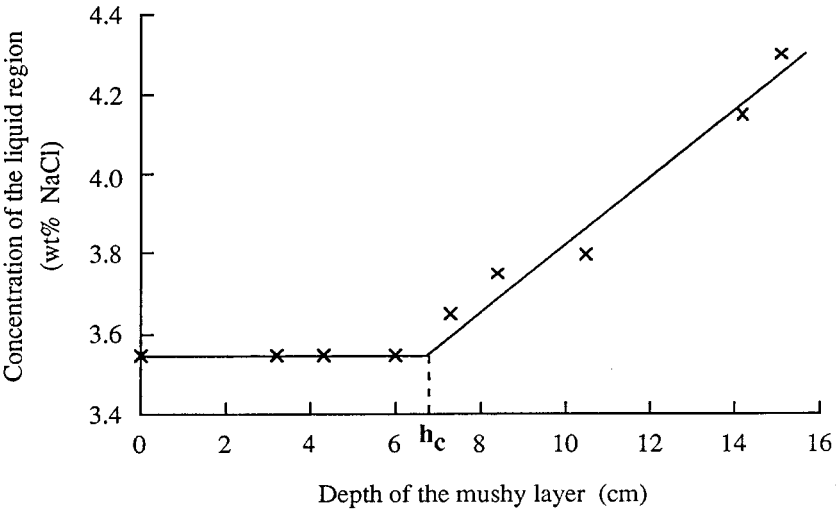

Figure 11 The composition of the liquid region below "sea ice" grown in a finite container filled with an aqueous solution of sodium chloride graphed as a function of the depth of the sea-ice layer. Initially, brine rejected by the growing ice crystals remains within the interstices of the sea ice. Once the depth of the layer exceeds a critical value h_c, which depends on the applied cooling rate, brine drains from the sea ice into the liquid below.

discard any turbine blade that shows evidence of freckling, which is enormously costly in terms of wasted production time and energy. There is yet much to be gained from a proper theoretical understanding of chimney formation backed up by simple laboratory experiments.

8. SUMMARY

Most of the theoretical work on mushy layers to date has been carried out by mathematical modelers concerned with the development of appropriate governing equations. A lot of the effort has been expended justifying the various assumptions and approximations made in their development. I have tried to present here a distillation of the mathematical models in a definition of an "ideal" mushy layer. The hope is that this will form a convenient starting point for further theoretical investigations so that convection in mushy layers becomes as well understood as Bénard convection of a Boussinesq fluid.

Some of the theoretical investigations performed so far have been described in this article. We have seen that the ideal mushy layer is rich in dynamical behavior, some anticipated and some wholly unexpected. The predicted

behavior of ideal mushy layers has been shown to be very similar to the behavior of a number of actual solidifying systems, so the study of ideal mushy layers is of practical benefit. Yet there is some observed behavior that is yet to be explained fully. Such explanations might come from further investigations of ideal mushy layers; others may come from extended models that incorporate nonideal effects.

ACKNOWLEDGMENTS

I am very grateful to many colleagues for discussions leading to improvements in this chapter including particularly DM Anderson, SH Davis, HE Huppert, RC Kerr, TP Schulze, HA Stone and JS Wettlaufer.

Literature Cited

Amberg G, Homsy GM. 1993. Nonlinear analysis of buoyant convection in binary solidification with application to channel formation. *J. Fluid Mech.* 252:79–98

Anderson DM, Worster MG. 1995. Weakly-nonlinear analysis of convection in a mushy layer during the solidification of binary alloys. *J. Fluid Mech.* 302:307–31

Anderson DM, Worster MG. 1996. A new oscillatory instability in a mushy layer during the solidification of binary alloys. *J. Fluid Mech.* 307:245–67

Bergman MI, Fearn DR. 1994. Chimneys on the Earth's inner-outer core boundary? *Geophys. Res. Lett.* 21(6):477–80

Burton WK, Cabrera N, Frank FC. 1951. The growth of crystals and the equilibrium structure of their surfaces. *Phil. Trans. Roy. Soc.* A243:299–358

Chadam J, Hoff D, Merino E, Ortoleva P, Sen A. 1986. Reactive infiltration instabilities *IMA J. Appl. Maths* 36:207–21

Chen CF. 1995. Experimental study of convection in a mushy layer during directional solidification. *J. Fluid Mech.* 293:81–98

Chen F, Chen CF. 1991. Experimental study of directional solidification of aqueous ammonium chloride solution. *J. Fluid Mech.* 227:567–86

Chen F, Lu JW, Yang TL. 1994. Convective instability in ammonium chloride solution directionally solidified from below. *J. Fluid Mech.* 276:163–87

Chiareli AOP, Huppert HE, Worster MG. 1994. Segregation and flow during the solidification of alloys. *J. Crystal Growth* 139:134–46

Chiareli AOP, Worster MG. 1995. Flow focusing instability in a solidifying mushy layer. *J. Fluid Mech.* 297:293–305

Copley SM, Giamei AF, Johnson SM, Hornbecker MF. 1970. The origin of freckles in binary alloys. *IMA J. Appl. Math.* 35:159–74

Davis SH. 1990. Hydrodynamic interactions in directional solidification. *J. Fluid Mech.* 212:241–62

Eide LI, Martin S. 1975. The formation of brine drainage features in young sea ice. *J. Glaciol.* 14(70):137–54

Emms PW. 1993. *Compositional convection and freckle formation in the solidification of binary alloys*. PhD thesis. Univ Oxford

Emms PW, Fowler AC. 1994. Compositional convection in the solidification of binary alloys. *J. Fluid Mech.* 262:111–39

Fearn DR, Loper DE, Roberts PH. 1981. Structure of the Earth's inner core. *Nature* 292:232–33

Fellicelli SD, Heinrich JC, Poirier DR. 1991. Simulation of freckles during vertical solidification of binary alloys. *Metall. Trans.* 22B:847–59

Flemings MC. 1974. *Solidification Processing.* New York:McGraw Hill.

Flemings MC, Nereo GE. 1967. Macrosegregation, part I. *Trans. Met. Soc. AIME* 239:1449–61

Fowler AC. 1985. The formation of freckles in binary alloys. *IMA J. Appl. Math.* 35:159–74

Fujii T, Poirier DR, Flemings MC. 1979. *Metall. Trans.* 10B:331–39

Ganesan S, Chan CL, Poirier DR. 1992. Permeability for flow parallel to primary dendrite arms. *Mat. Sci. Eng.* A151:97–105

Glicksman ME, Coriell SR, McFadden GB. 1986. Interaction of flows with the crystal-melt interface. *Annu. Rev. Fluid Mech.* 18:307–35

Hills RN, Loper DE, Roberts PH. 1983. A thermodynamically consistent model of a mushy zone. *Q. J. Mech. Appl. Math.* 36:505–39

Hinch EJ, Bhatt BS. 1990. Stability of an acid front moving through porous rock. *J. Fluid Mech.* 212:279–88

Horton CW, Rogers FT. 1945. Convection currents in a porous medium. *J. Appl. Phys.* 16:367–70

Huppert HE. 1990. The fluid mechanics of solidification. *J. Fluid Mech.* 212:209–40

Huppert HE, Hallworth MA. 1993. Solidification of NH_4Cl and NH_4Br from aqueous solutions contaminated by $CuSO_4$: the extinction of chimneys. *J. Crystal Growth* 130:495–506

Huppert HE, Worster MG. 1985. Dynamic solidification of a binary melt. *Nature* 314:703–7

Hurle DTJ. 1992. Morphological stability and convective flow: some old and new problems. In *Interactive Dynamics of Convection and Solidification*, ed. SH Davis, HE Huppert, U Müller, MG Worster, NATO ASI Ser. E219:1–14. Dordrecht: Kluwer

Jenkins A, Bombosch A. 1995. Modeling the effects of frazil ice crystals on the dynamics and thermodynamics of Ice Shelf Water plumes. *J. Geophys. Res.* 100 C4:6967–81

Kerr RC, Tait S. 1986 Crystallization and compositional convection in a porous medium with application to layered igneous intrusions. *J. Geophys. Res.* 91:3591–608

Kerr RC, Woods AW, Worster MG, Huppert HE. 1990. Solidification of an alloy cooled from above. Part 2. Nonequilibrium interfacial kinetics. *J. Fluid Mech.* 217:331–48

Langlois WE. 1985. Buoyancy-driven flows in crystal growth melts. *Annu. Rev. Fluid Mech.* 17:191–215

Lapwood ER. 1948. Convection of a fluid in a porous medium. *Proc. Cambridge Phil. Soc.* 44:508–21

Martin S. 1981. Frazil ice in rivers and oceans. *Annu. Rev. Fluid Mech.* 13:379–97

Mehrabian R, Keane M, Flemings MC. 1970. Interdendritic fluid flow and macrosegregation: influence of gravity. *Metall. Trans.* 1:1209–20

Mellor JW. 1981. *A Comprehensive Treatise on Inorganic and Theoretical Chemistry*, 7:383–89. London: Longmans

Moffat HK, Loper DE. 1994. The magnetospheric rise of a buoyant parcel in the Earth's core. *Geophys. J. Int.* 117:394–402

Mullins WW, Sekerka RF. 1964. Stability of a planar interface during solidification of a binary alloy. *J. Appl. Phys.* 35:444–51

Nandapurkar P, Poirier DR, Heinrich JC, Felicelli S. 1989. Thermosolutal convection during dendritic solidification of alloys: Part 1. Linear stability analysis. *Metall. Trans.* 20B:711–21

Ni J, Beckermann C. 1991. A volume-averaged two-phase model for transport phenomena during solidification. *Metall. Trans.* 22B:349–61

Palm E, Weber JE, Kvernvold O. 1972. On steady convection, in a porous medium. *J. Fluid Mech.* 54:153–61

Petersen JS. 1987. Crystallization shrinkage in the region of partial solidification: implications for silicate melts. In *Structure and Dynamics of Partially Solidified Systems*, ed. DE Loper, NATO ASI Ser. E125:417–35. Dordrecht:Martinus Nijhoff

Phillips OE. 1991. *Flow and Reactions in Permeable Rocks*. Cambridge: Cambridge University Press

Raz E, Lipson SG, Ben-Jacob E. 1991. New periodic morphologies observed during dendritic crystal growth of ammonium choloride crystals in thin layers. *J. Crystal Growth* 108:637–46

Roberts P, Loper DE. 1983. Towards a theory of the structure and evolution of a dendrite layer. In *Stellar and Planetary Magnetism*, ed. AM Soward, pp. 329–49. New York: Gordon Breach

Sample AK, Hellawell A. 1984. The mechanisms of formation and prevention of channel segregation during alloy solidification. *Metall. Trans.* 15A:2163–73

Sarazin JR, Hellawell A. 1988. Channel formation in Pb-Sn, Pb-Sb and Pb-Sn-Sb alloys and comparison with the system NH_4Cl-H_2O. *Metall. Trans.* 19A:1861–71

Schneider MC, Beckermann C. 1992. Simulation of the columnar dendritic solidification of a Pb-Sn alloy. In *Interactive Dynamics of Convection and Solidification*, ed. SH Davis, HE Huppert, U Müller, MG Worster, NATO ASI Ser. E219:195–97. Dordrecht: Kluwer

Sherwood JD. 1987. Stability of a plane reaction front in a porous medium. *Chem. Eng. Sci.* 42(7):1823–29.

Tait S, Jahrling K, Jaupart C. 1992. The planform of compositional convection and chimney formation in a mushy layer. *Nature* 359:406–8

Tait S, Jaupart C. 1989. Compositional convection in viscous melts. *Nature* 338:571–74

Tait S, Jaupart C. 1992. Compositional con-

vection in a reactive crystalline mush and the evolution of porosity. *J. Geophys. Res.* 97:6735–56

Tait S, Kerr RC. 1987. Experimental modelling of interstitial melt convection in cumulus piles. In *Origins of Igneous Layering*, ed. I Parsons, pp. 569–87. Dordrecht: Reidel

Turner JS. 1979. *Buoyancy Effects in Fluids*. Cambridge: Cambridge Univ. Press

Turner JS. 1985. Multicomponent convection. *Annu. Rev. Fluid Mech.* 17:11–44

Worster MG. 1986. Solidification of an alloy from a cooled boundary. *J. Fluid Mech.* 167:481–501

Worster MG. 1990. Structure of a convecting mushy layer. *Appl. Mech. Rev.* 43(5):S59–62

Worster MG. 1991. Natural convection in a mushy layer. *J. Fluid Mech.* 224:335–59

Worster MG. 1992a. The dynamics of mushy layers. In *Interactive Dynamics of Convection and Solidification*, ed. SH Davis, HE Huppert, U Müller, MG Worster, NATO ASI Ser. E219:113–38. Dordrecht: Kluwer

Worster MG. 1992b. Instabilities of the liquid and mushy regions during solidification of alloys. *J. Fluid Mech.* 237:649–69

Worster MG, Kerr RC. 1994. The transient behavior of alloys solidified from below prior to the formation of chimneys. *J. Fluid Mech.* 269:23–44

Annual Review of Fluid Mechanics
Volume 29, 1997

CONTENTS